Electronic Supplementary Material (ESI) for Organic & Biomolecular Chemistry.

SUPPORTING INFORMATION

Instrumentation and methods

NMR spectroscopy.

^{1}H and ^{13}C spectra were recorded with a 400 MHz bruker Avance 400 instrument. The chemical shifts (δ) are indicated in ppm with respect to an internal reference corresponding to the references of deuterated solvents ($CDCl_3$: 7.26 ppm; CD_3OD: 3.31 ppm; CD_3CN: 1.94 ppm; $(CD_3)_2CO$: 2.05 ppm for ^{1}H-NMR and $CDCl_3$: 77.16 ppm; CD_3OD: 49.00 ppm; CD_3CN: 1.31 and 118.26 ppm; $(CD_3)_2CO$: 29.84 and 206.26 ppm for ^{13}C-NMR). The attributions are given in the following manner: chemical shift followed in bracket: multiplicity of the signal (s, d, t, q, m, dd, et dq corresponding respectively to singlet, doublet, triplet, quadruplet, multiplet, double doublet and double quadruplet), coupling constant in Hz, and number of protons.

Mass spectrometry.

LCMS analysis were realized using an Agilent 1200 SL/QTof 6520 spectrometer coupled to a Hypersil Gold C18 column with 1.9 μm particles size and 1x30 mm dimensions. ESI mass spectra were obtained using an Agilent 1200 SL spectrometer MicroTOF (Bruker®) equipped with an electrospray source.

UV-Visible absorption and emission spectroscopy.

UV-visible absorption spectra were measured using a double beam spectrophotometer UVIKON XS.

Fluorescence emission spectra were obtained using a spectrofluorometer fluoroMax from Horiba-Jobin Yvon.

Fluorescence quantum yields were measured by the relative method, using quinine sulfate as reference.[1,2] The absorbance of the samples and the reference were chosen so that they were in the 0.1-0.15 range and nearly identical at the same excitation wavelength. Emission quantum yields were then calculated according to the method described by Crosby and Demas, taking into account the differences between the refractive indices of the sample and reference solutions.[3]

Micro-wave.

The pallado-catalyzed reactions were performed using an Anton Paar Monowave 300.

Chromatography.

Thin Layer Chromatography (TLC) were realized using plates covered with silica gel 60 F254 Merck.

Column chromatography were performed on silica gel 60 (230-400 mesh, 0,040-0,063 mm) Merck.

High Performance Liquid Chromatography (HPLC).

Analytical HPLC were realized over a series of high performance chromatography Waters® (Waters 600 double body pumps with diode detector Dionex UVD340V or Waters 1525 pump with Waters 2996 detector) equipped with Phenomenex C18 PolarRP 4-micron (4.6, 250 mm) analytical columns, Thermo Betabasic 5-micron (4.6, 250 mm) analytical columns, Agilent Zorbax SB-C18 5-microns (4.6, 250 mm) columns or Kromasil 100-5C18 (4.6, 250 mm)

columns. The HPLC analyses were done using a gradient starting from 100% mQ H_2O acidified with 0.01% of TFA and reaching 100% of acetonitrile in 30 min.
Preparative HPLC were realized over a series of high performance chromatography Waters® (Waters 600 double body pumps with diode detector Dionex UVD340V equipped with a semi-preparative Phenomenex C18 PolarRP 10-micron (10, 250 mm) column, Thermo Betabasic 5-micron (10, 250 mm) column, ou Kromasil 100-5C18 (10, 250 mm) column. These purifications were done using an isocratic solvent elution.

Solvents et reagents.

Reagents and anhydrous solvents used for the synthesis were ordered at Sigma-Aldrich, Alfa Aesar, TCI EUROPE or Acros Organics. All commercial reagents were used for the synthesis without any further purification. Tetrahydrofuran used in the reactions was freshly distilled using sodium metal and benzophenone.

Irradiation procedure:

The same irradiation procedure was followed for the irradiations of **6**,**7a-c** and **11**:
A 2 mL solution of **6** (135 μM), **7a** (100 μM), **7b** (60 μM), **7c** (75 μM) and **11** (40 μM) in 0.1 mM pH 7.4 phosphate buffer/acetonitrile (1/1 v/v) was exposed to a LUMOS 43 LED source (Atlas Photonics Inc.) at 405 nm (Typical optical output: 200 mW/cm^2). The reaction was monitored by UV and aliquots of samples (100 μL) were analyzed by HPLC to determine the percentage of released 3,4-dimethoxyphenylacetic acid (MPAA) using a calibration curve (Figure S33).

UV-Visible monitoring of photolysis.

The irradiations were monitored by UV-visible spectroscopy by measuring the absorbance at each irradiation time using a using a double beam spectrophotometer UVIKON XS with acetonitrile as a blank between 250 and 750 nm.

FTIR study of the photolysis.

A sample of compound **7b** was prepared in acetonitrile (C = 267 μM). The solution was irradiated using the LUMOS 43 LED source (Atlas Photonics Inc.) at 405 nm (Typical optical output: 200 mW/cm^2) for 40 minutes. The infrared spectra of the starting material and the photolysis products were recorded on a brucker FT-IR ALPHA.

NMR protocol for the study of the photolytical reaction:

Two samples of compound **6** were prepared in deuterated acetonitrile (CD_3CN) with respective concentrations of 267 μM and 405 μM. The samples were irradiated at 405 nm for 90 minutes and 150 minutes respectively and their NMR spectra were recorded immediately. The acquisitions for the NMR spectra were recorded on a 500 MHz Bruker Avance II and ^{1}H NMR spectra were recorded at 500 MHz. This spectrometer is equipped with a dual cryoprobe ^{1}H/^{13}C (5 mm cryoprobe double resonance probe fixed frequency DCH ^{13}C/^{1}H/D z-grad)

Fluorescence on cells.

Studies on cell culture were performed on HeLa cells. HeLa cells were cultured in DMEM complete culture medium containing phenol red at 37°C with 5% CO_2. They were seeded and maintained in 25 mL Falcon culture flask or multi well LabTek (Lab-Tek® II) culture flasks. The imaging experiments were performed in IBIDI 60 □-Dish. Confocal images were obtained on a Leica DMI4000B TSP SPE microscope. Photolysis was performed on the same microscope stand with using a Leica EL6000 light source with a DAPI filter cube (ex. 340-380 nm; dicroïc 400 nm; em. LP 425 nm) in epifluorescence mode. An average power of few tenth of mW was used to expose the specimen.

NMR Spectra / HPLC chromatograms

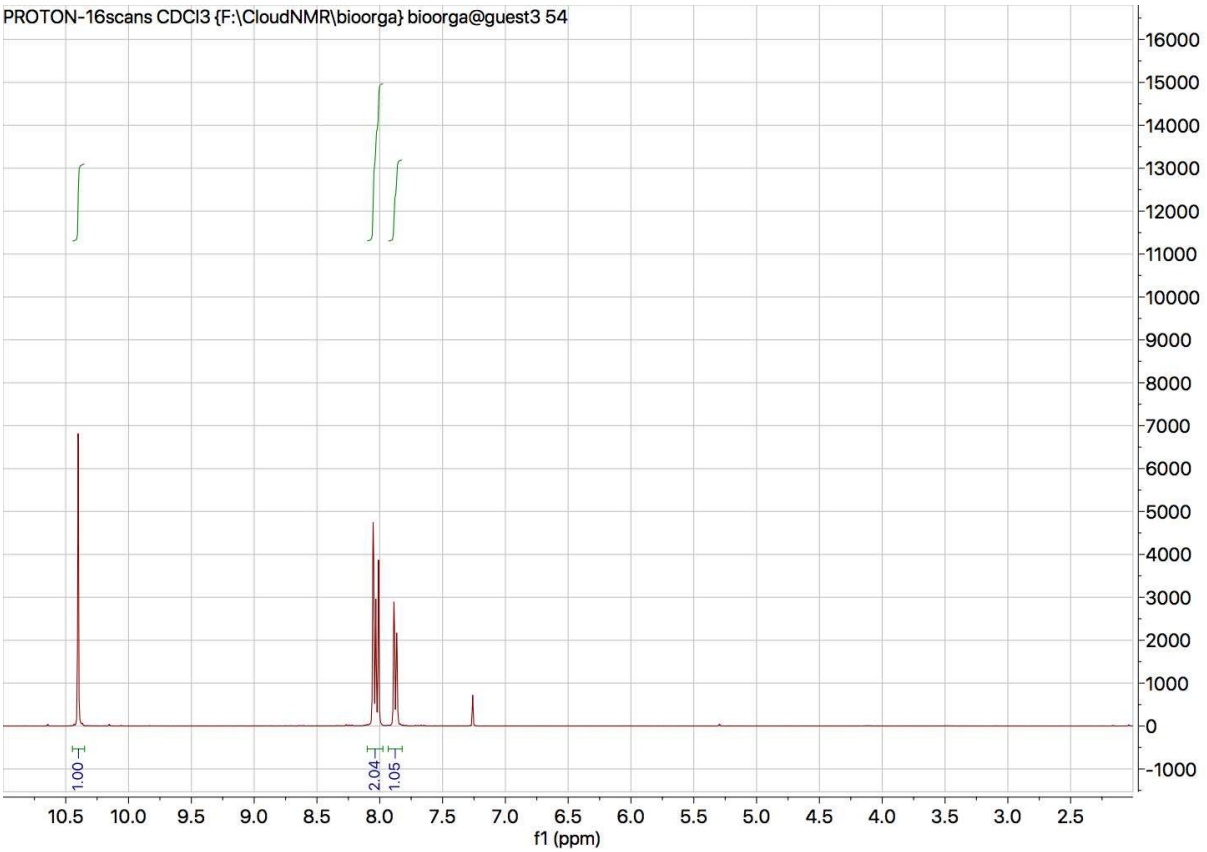

Figure S1: ^{1}H NMR spectrum of nitro-3-bromo-benzaldehyde (**2**).

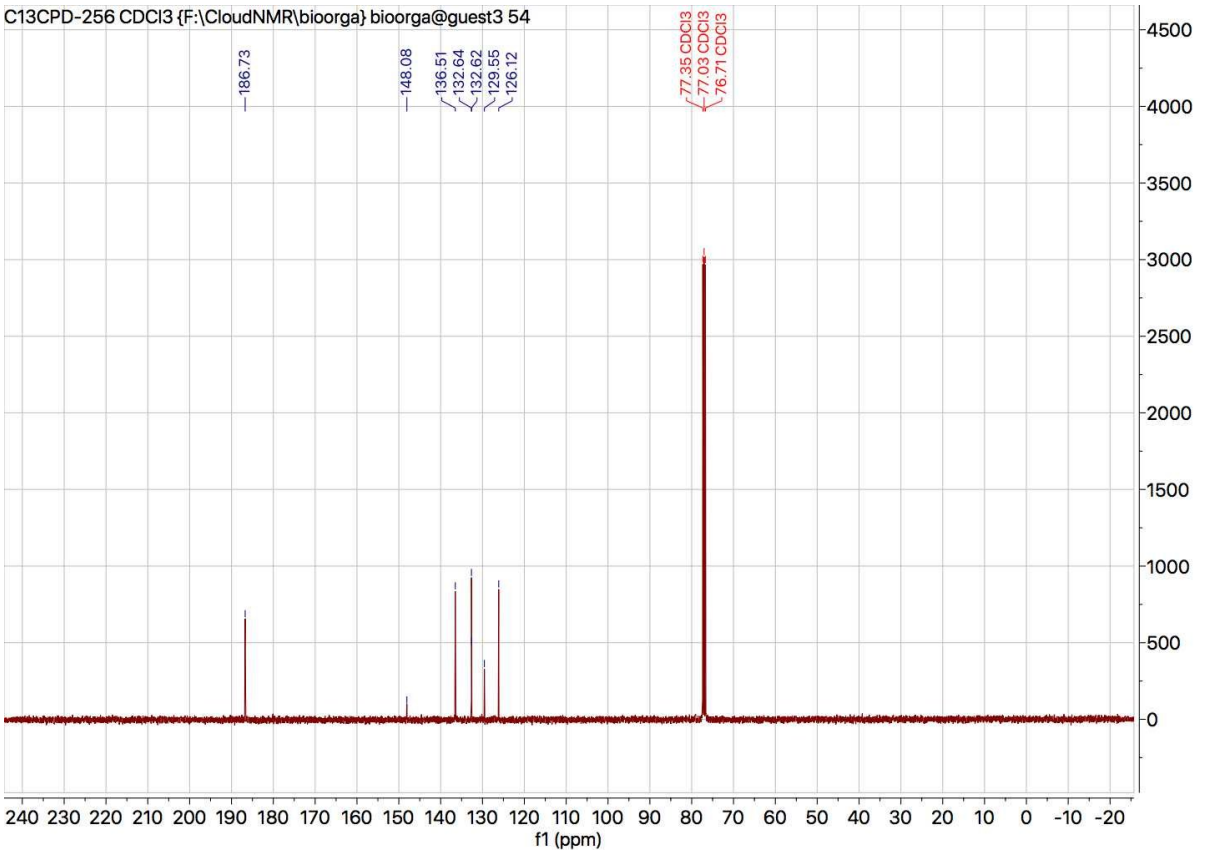

Figure S2: ^{13}C NMR spectrum of nitro-3-bromo-benzaldehyde (**2**).

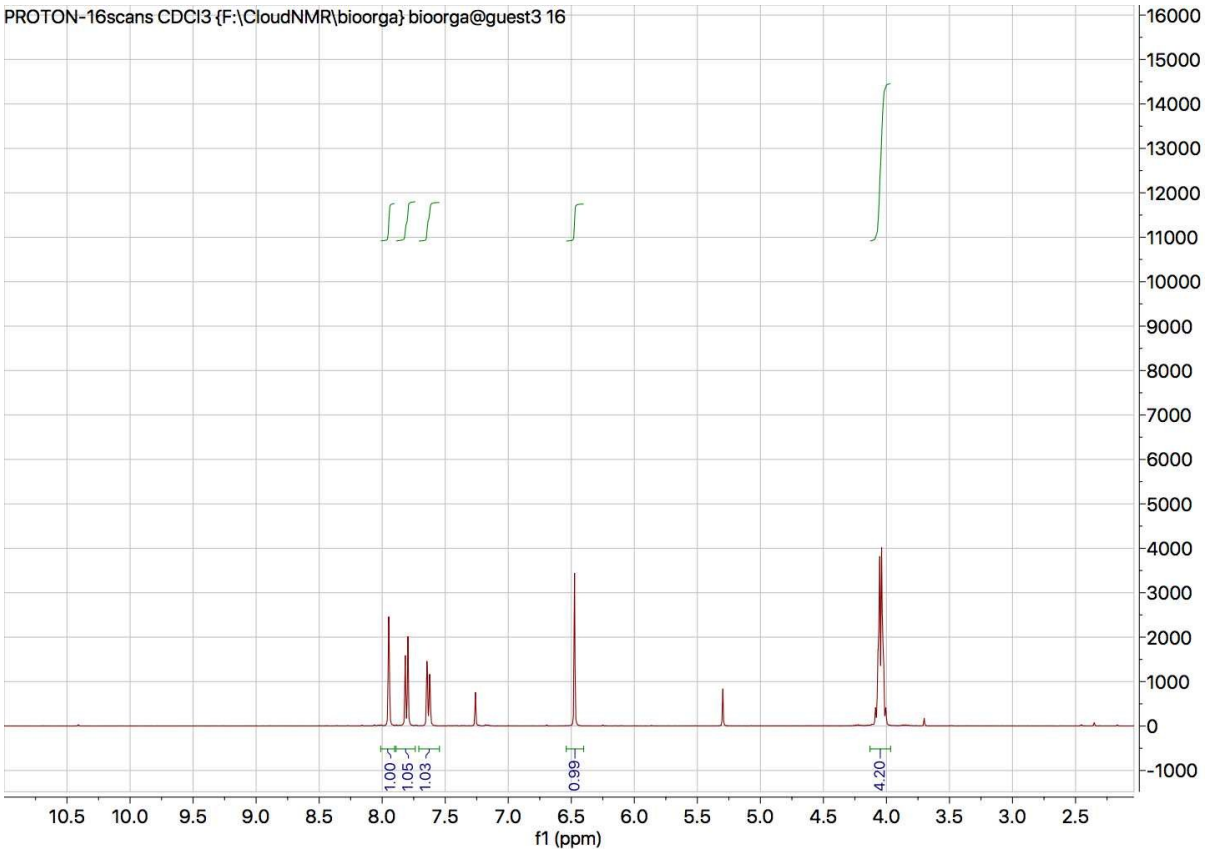

Figure S3: ^{1}H NMR spectrum of 2-(5-bromo-2-nitrophenyl)-1,3-dioxolane (**3**).

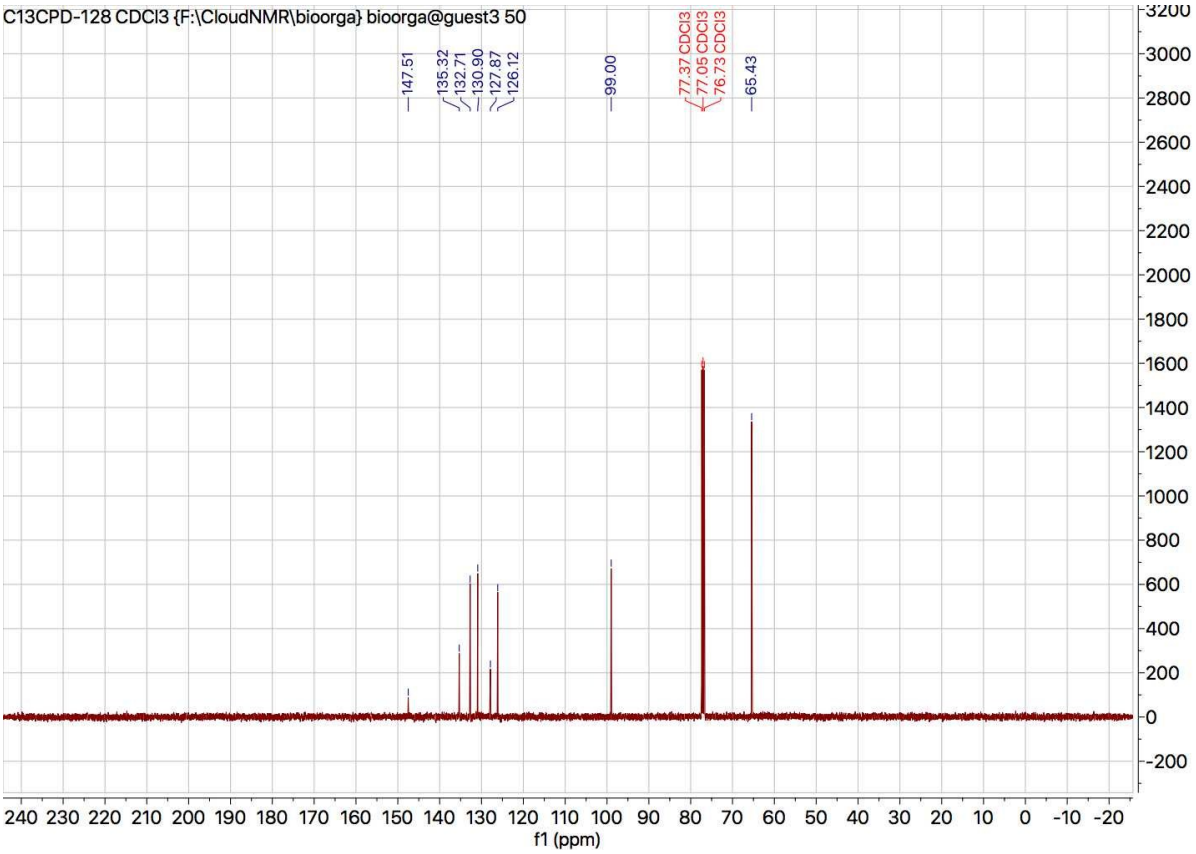

Figure S4: ^{13}C NMR spectrum of 2-(5-bromo-2-nitrophenyl)-1,3-dioxolane (**3**).

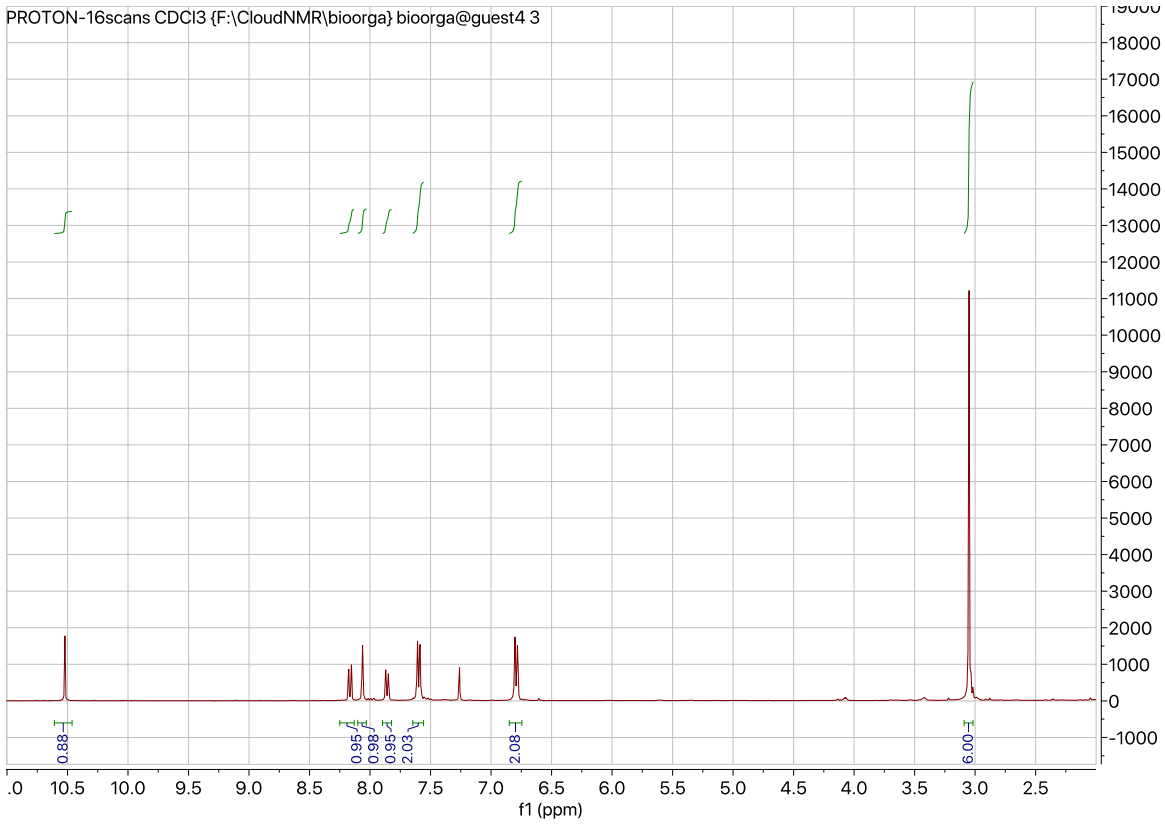

Figure S5: ^{1}H NMR spectrum of 4'-(dimethylamino)-4-nitro-(1,1'-biphenyl)-3-carbaldehyde (**4**).

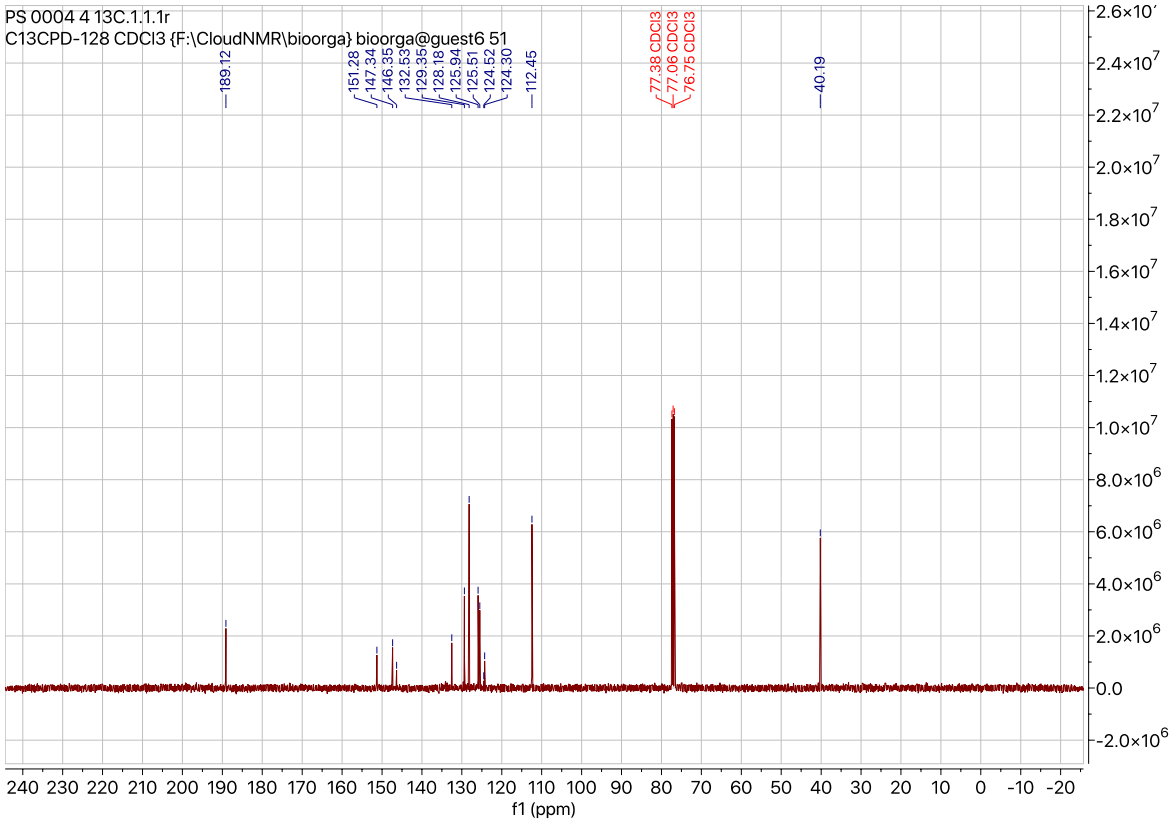

Figure S6: ^{13}C NMR spectrum of 4'-(dimethylamino)-4-nitro-(1,1'-biphenyl)-3-carbaldehyde (**4**).

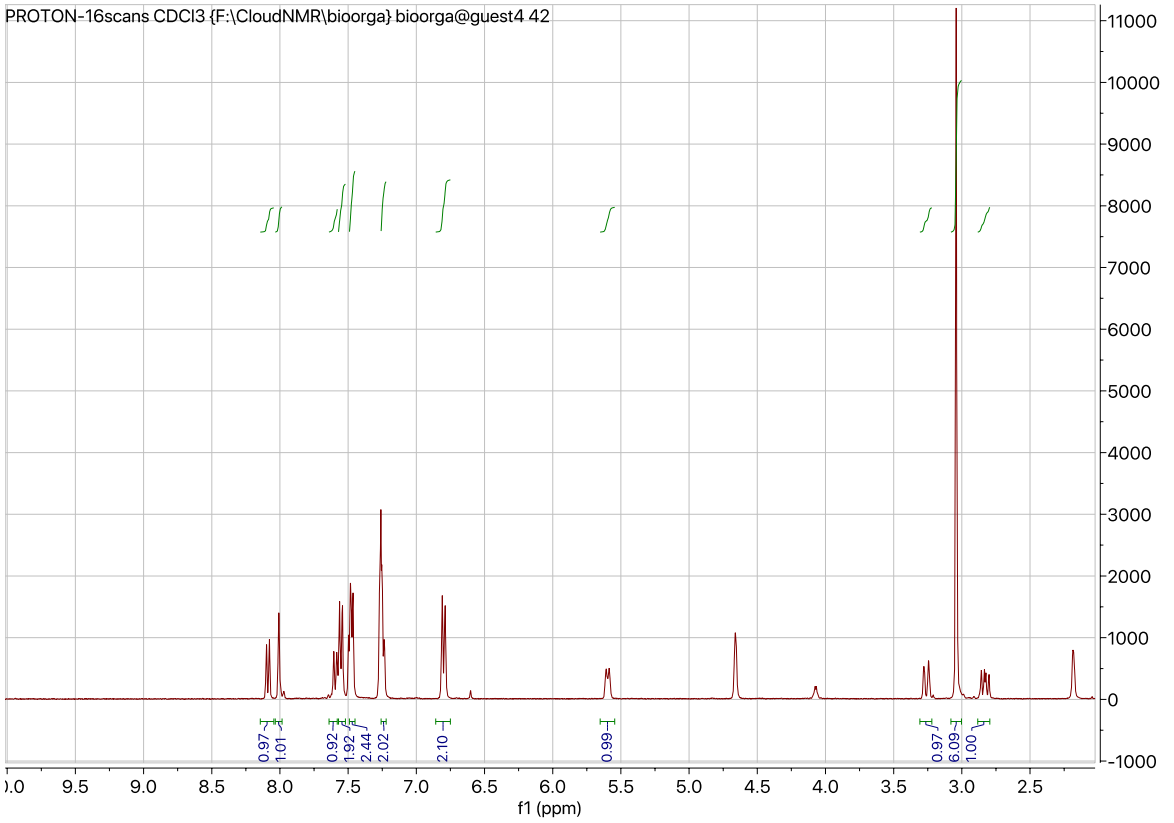

Figure S7: ^{1}H NMR spectrum of 2-(4-bromophenyl)-1-(4'-(dimethylamino)-4-nitro-(1,1'-biphenyl)-3-yl) ethan-1-ol (**5**).

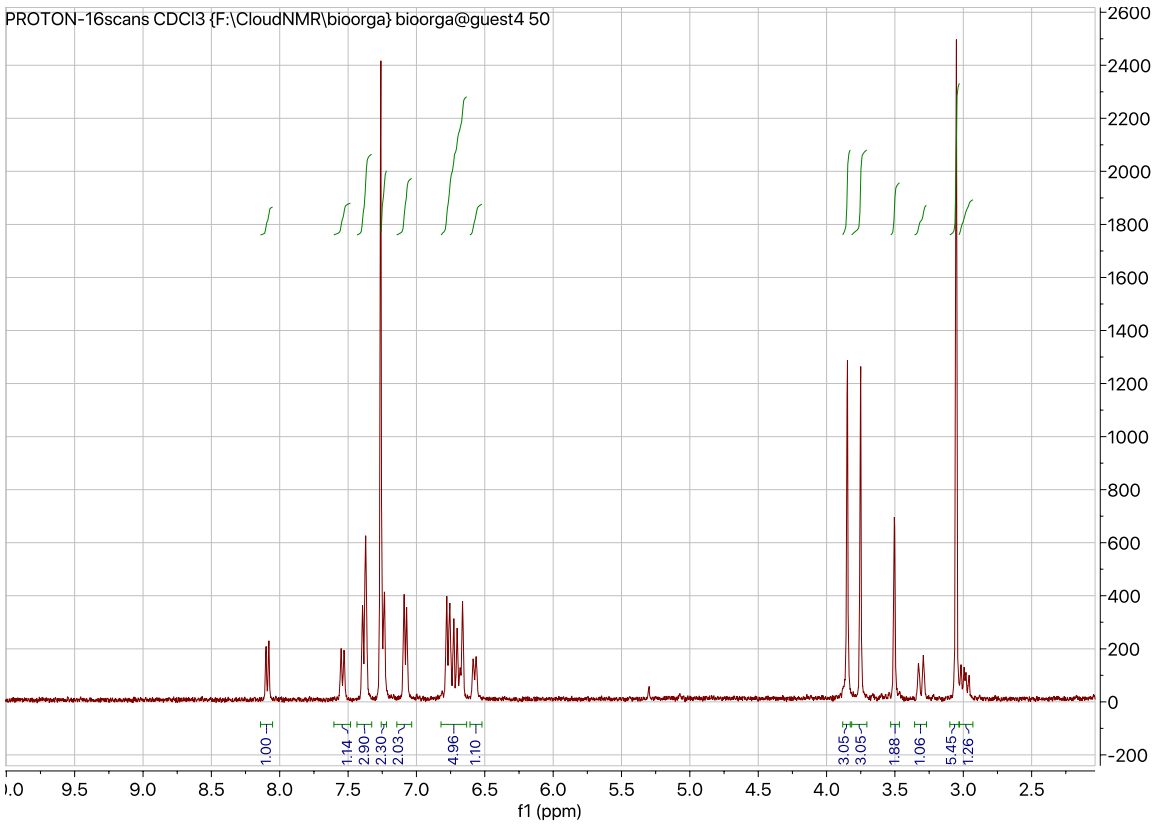

Figure S8: ^{1}H NMR spectrum of 2-(4-bromophenyl)-1-(4'-(dimethylamino)-4-nitro-(1,1'-biphenyl)-3-yl) ethyl 2-(3,4-dimethoxyphenyl)acetate (**6**).

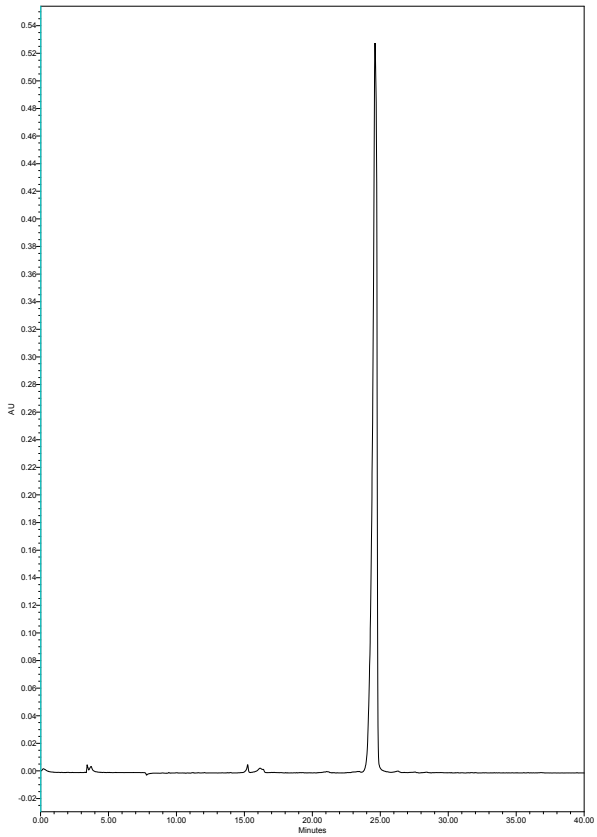

Figure S9: HPLC chromatogram profile of 2-(4-bromophenyl)-1-(4'-(dimethylamino)-4-nitro-(1,1'-biphenyl)-3-yl) ethyl 2-(3,4-dimethoxyphenyl)acetate (**6**).

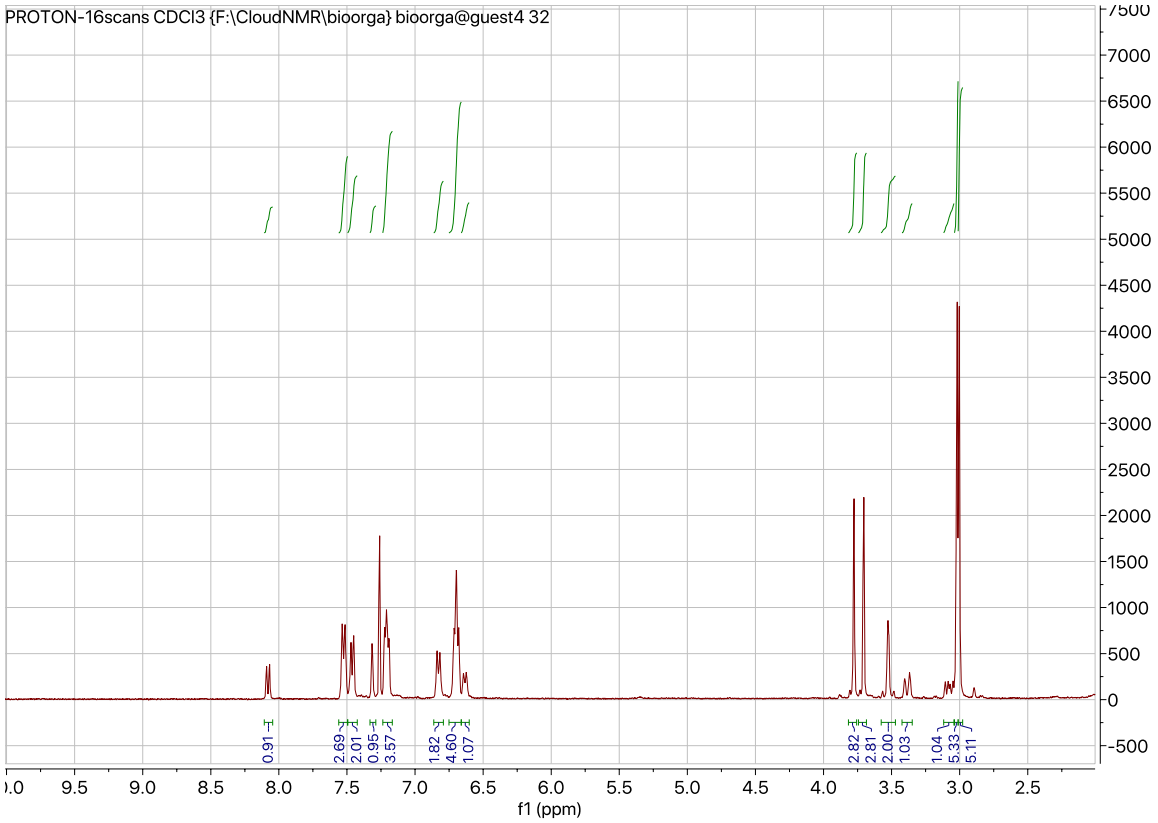

Figure S10: ^{1}H NMR spectrum of 1-(4'-(dimethylamino)-4-nitro-(1,1'-biphenyl)-3-yl)-2-(4'-(dimethylamino)-(1,1'-biphenyl)-4-yl) ethyl 2-(3,4 dimethoxyphenyl)acetate (**7a**).

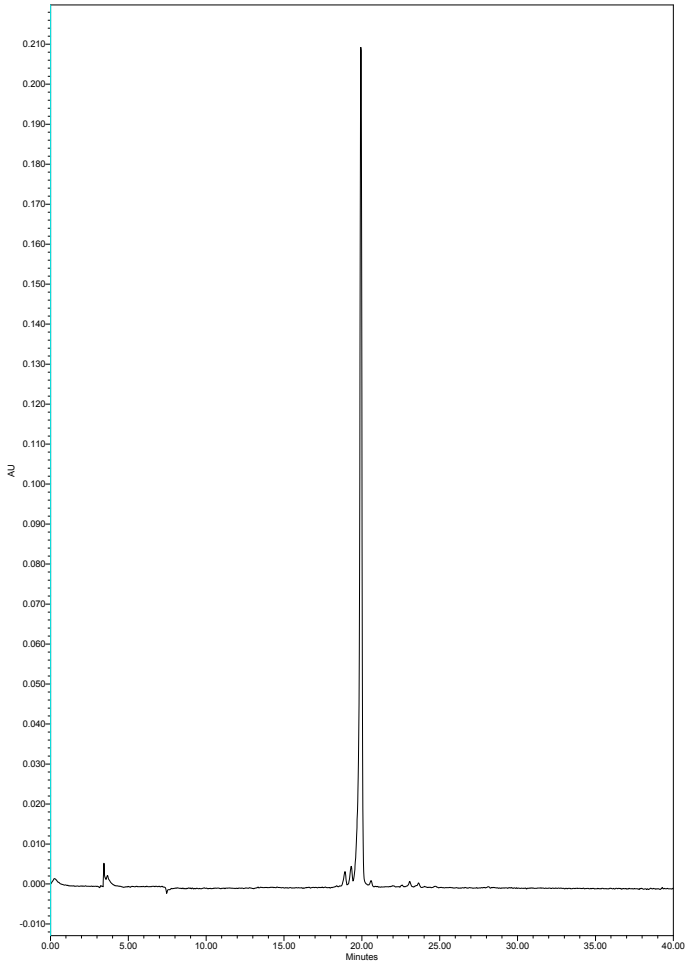

Figure S11: HPLC chromatogram profile of 1-(4'-(dimethylamino)-4-nitro-(1,1'-biphenyl)-3-yl)-2-(4'-(dimethylamino)-(1,1'-biphenyl)-4-yl) ethyl 2-(3,4 dimethoxyphenyl)acetate (**7a**).

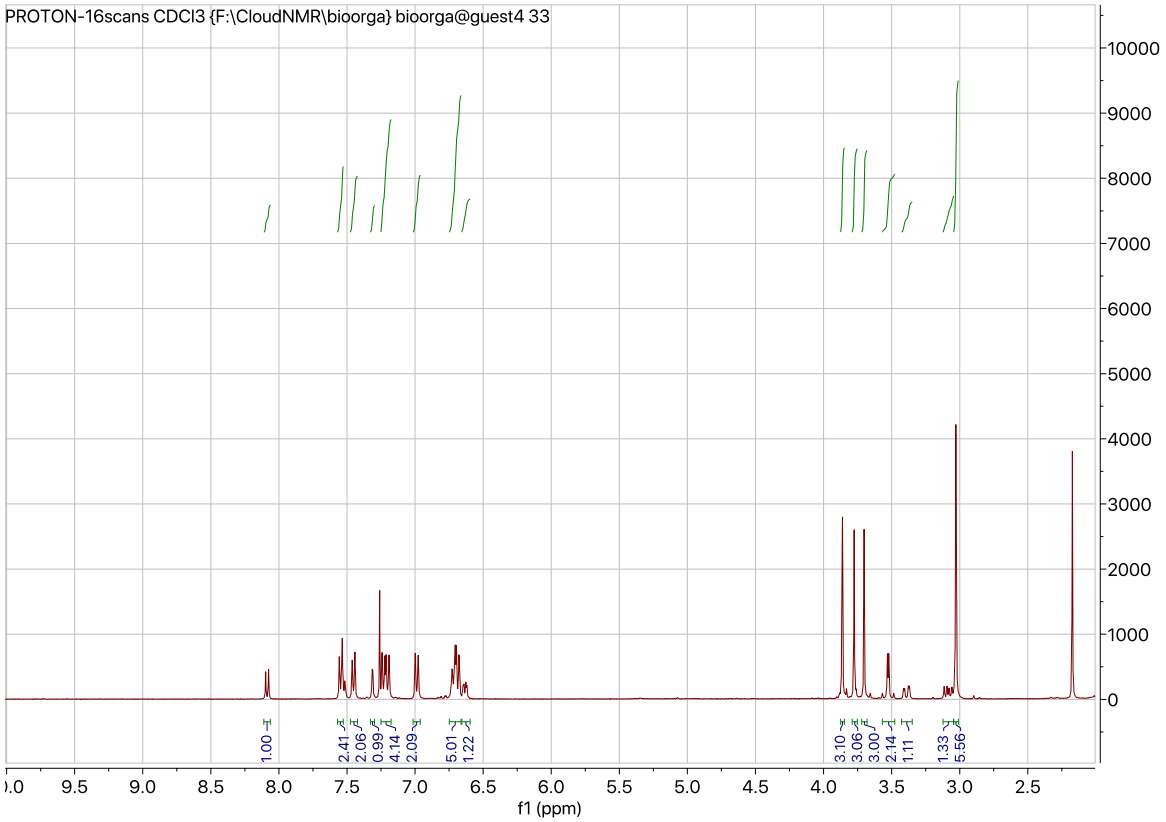

Figure S12: ^{1}H NMR spectrum of 1-(4'-(dimethylamino)-4-nitro-(1,1'-biphenyl)-3-yl)-2-(4'-methoxy (1,1'-biphenyl)-4-yl) ethyl 2-(3,4-dimethoxyphenyl) acetate (**7b**).

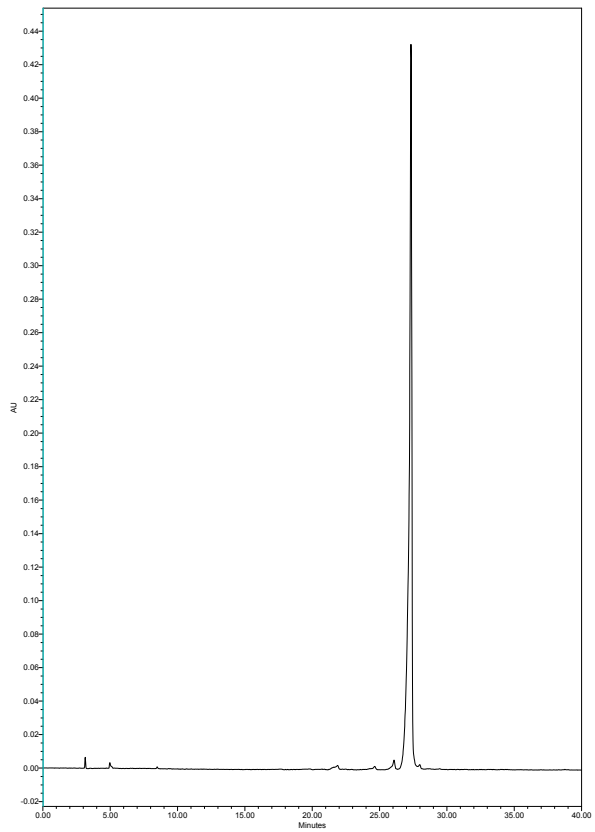

Figure S13: HPLC chromatogram profile of 1-(4'-(dimethylamino)-4-nitro-(1,1'-biphenyl)-3-yl)-2-(4'-methoxy (1,1'-biphenyl)-4-yl) ethyl 2-(3,4-dimethoxyphenyl) acetate (**7b**).

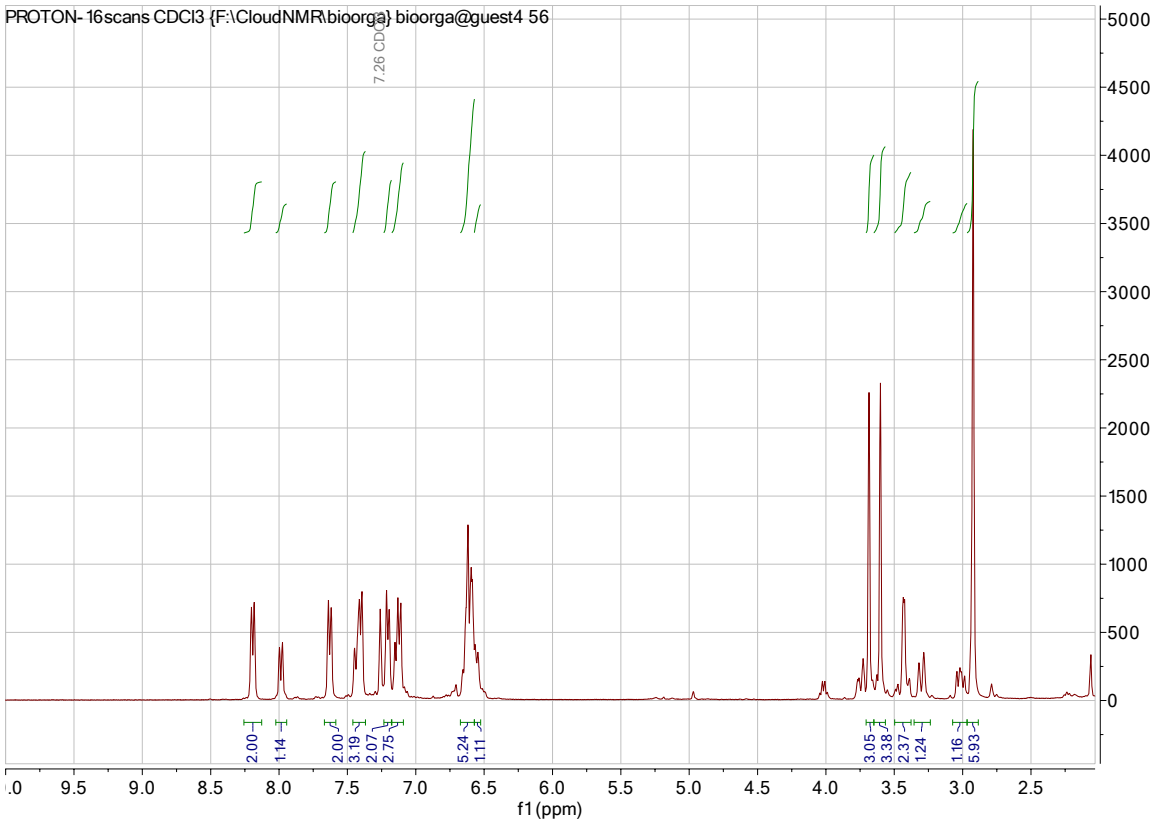

Figure S14: ^{1}H NMR spectrum of 1-(4'-(dimethylamino)-4-nitro-(1,1'-biphenyl)-3-yl)-2-(4'-nitro-(1,1'-biphenyl)-4-yl) ethyl 2-(3,4-dimethoxyphenyl) acetate (**7c**).

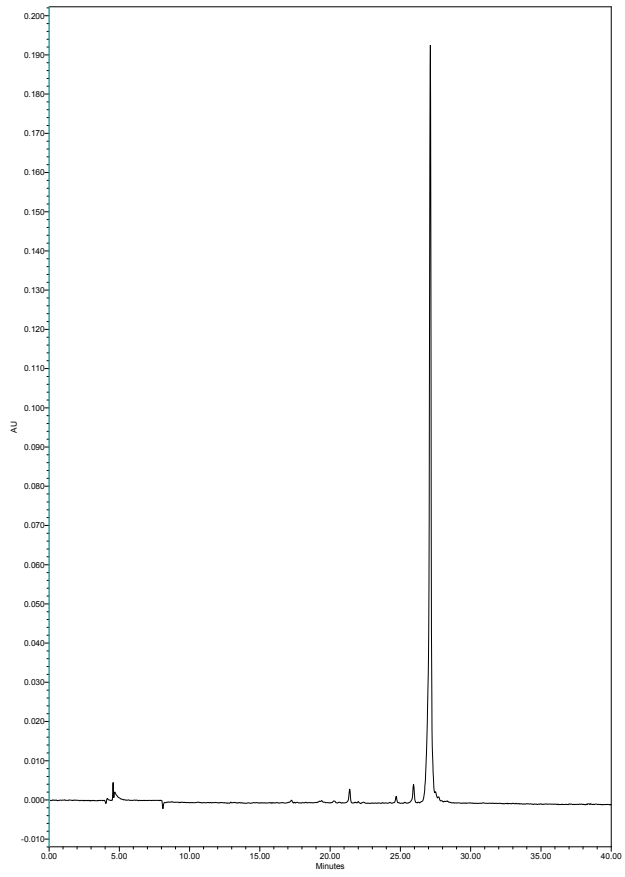

Figure S15: HPLC chromatogram profile of 1-(4'-(dimethylamino)-4-nitro-(1,1'-biphenyl)-3-yl)-2-(4'-nitro-(1,1'-biphenyl)-4-yl) ethyl 2-(3,4-dimethoxyphenyl) acetate (**7c**).

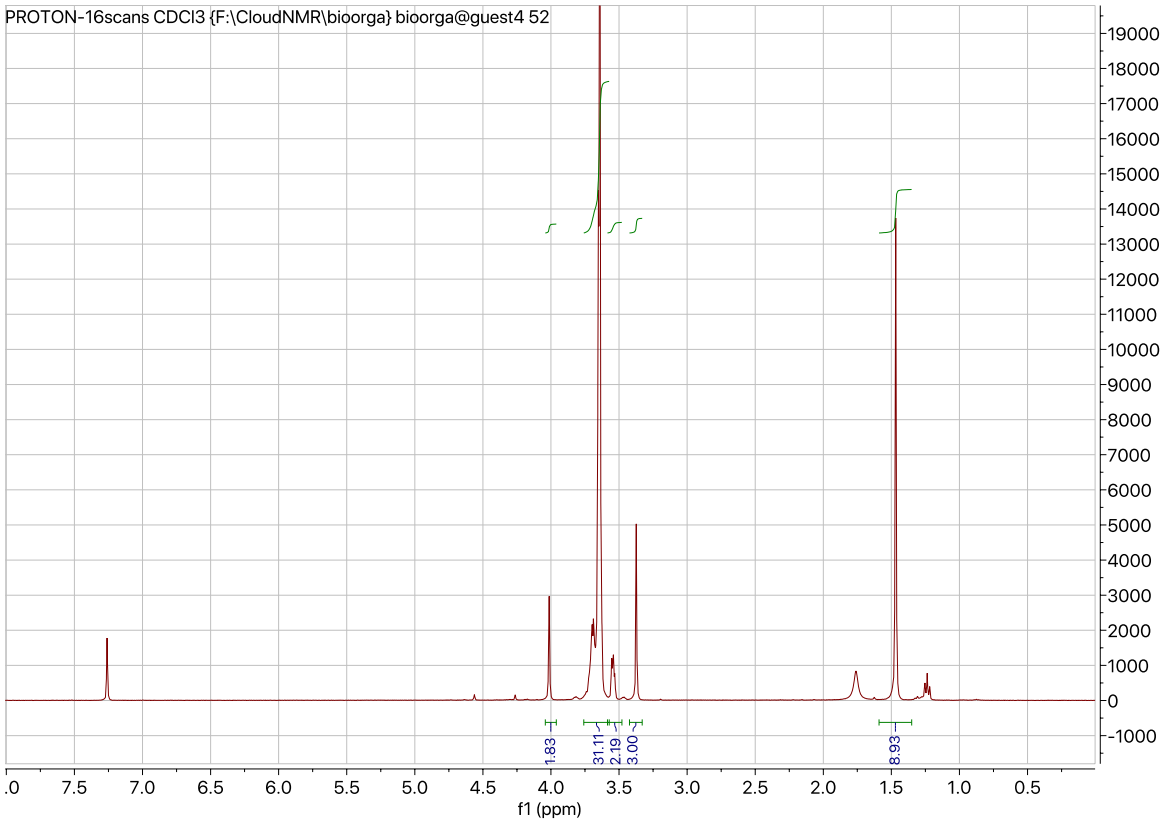

Figure S16: ^{1}H NMR spectrum of tert-butyl-2-(2-methoxyoctaethoxy) acetate (**8**).

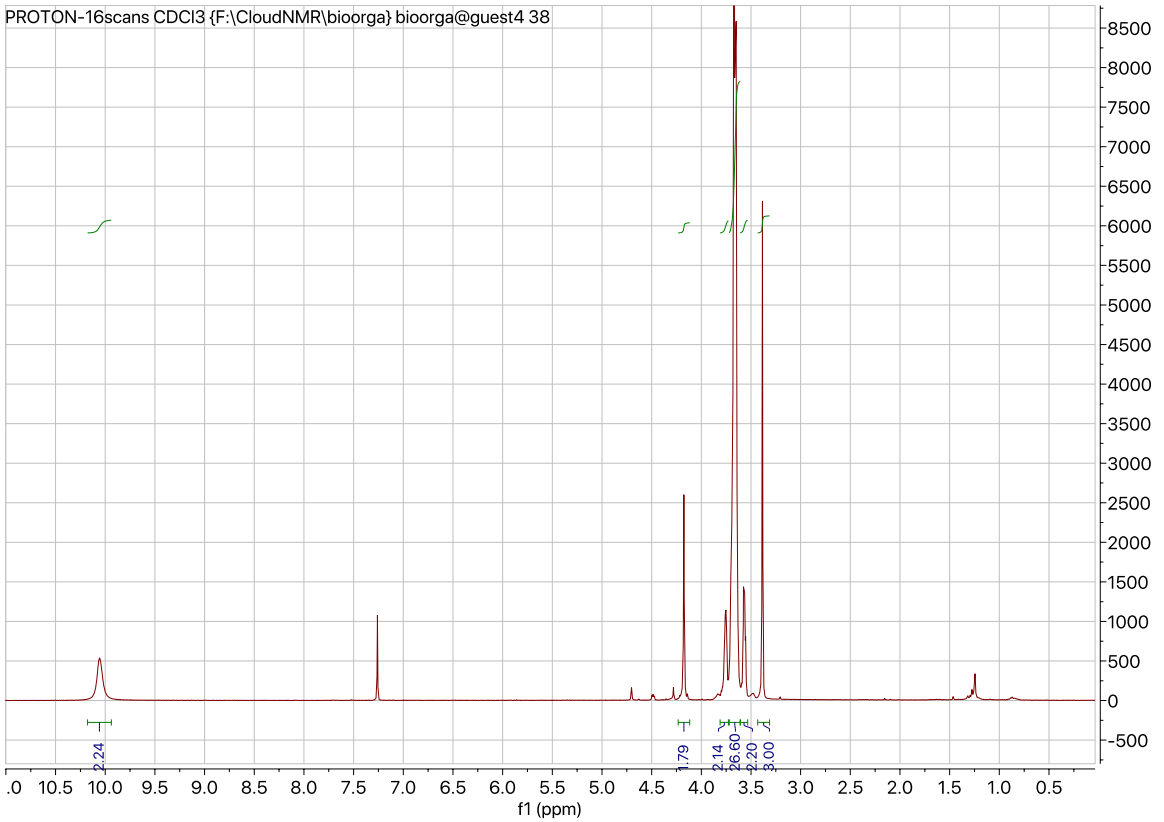

Figure S17: ^{1}H NMR spectrum of 2-(2-methoxyoctaethoxy)acetic acid (**9**).

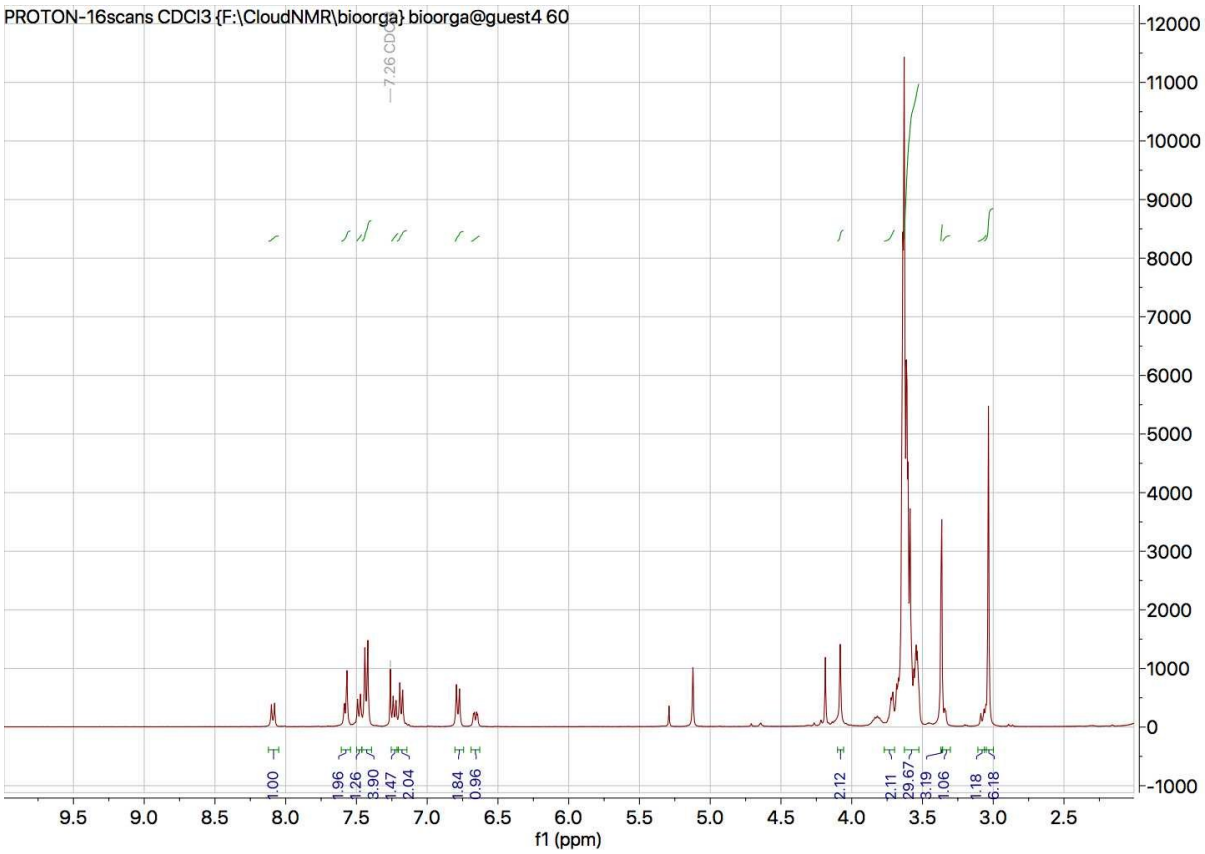

Figure S18: ^{1}H NMR spectrum of 2-(4-bromophenyl)-1-(4'-(dimethylamino)-4-nitro-(1,1'-biphenyl)-3-yl) ethyl 2-(2-methoxyoctaethoxy) acetate (**10**).

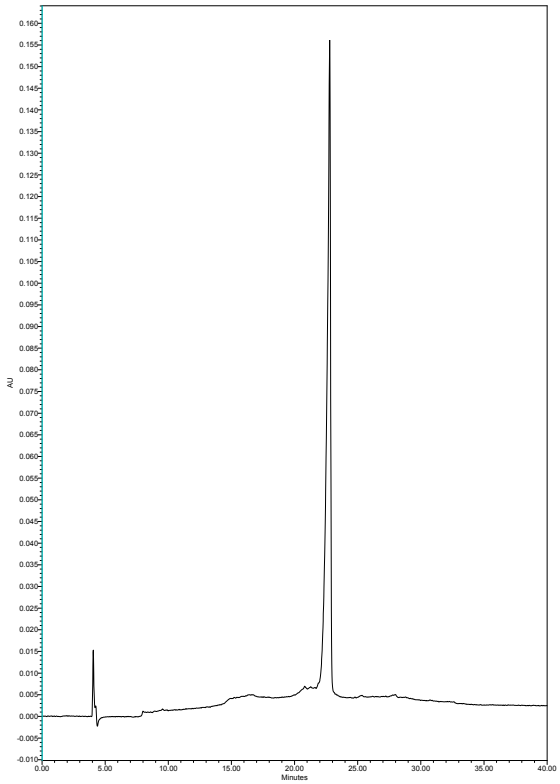

Figure S19: HPLC chromatogram profile of 2-(4-bromophenyl)-1-(4'-(dimethylamino)-4-nitro-(1,1'-biphenyl)-3-yl) ethyl 2-(2-methoxyoctaethoxy) acetate (**10**).

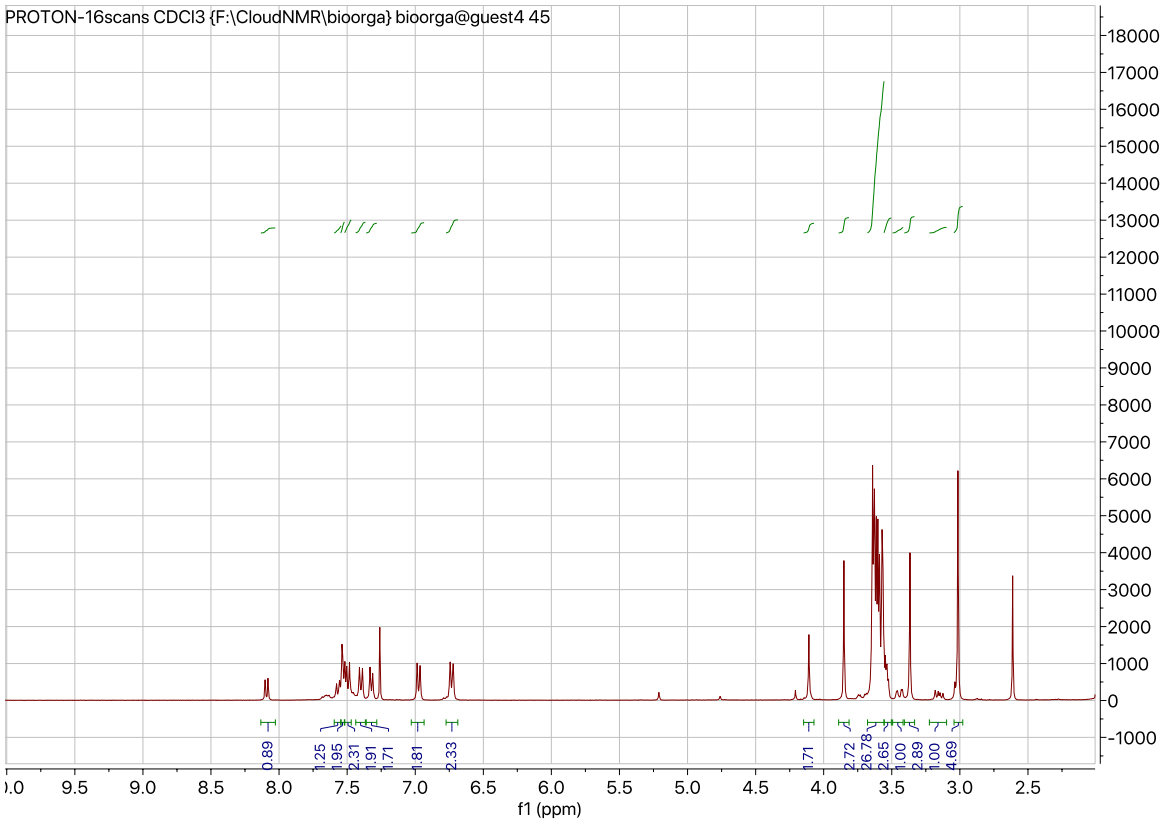

Figure S20: ^{1}H NMR spectrum of 1-(4'-(dimethylamino)-4-nitro-(1,1'-biphenyl)-3-yl)-2-(4'-methoxy-(1,1'-biphenyl)-4-yl) ethyl 2-(2-methoxyoctaethoxy) acetate (**11**).

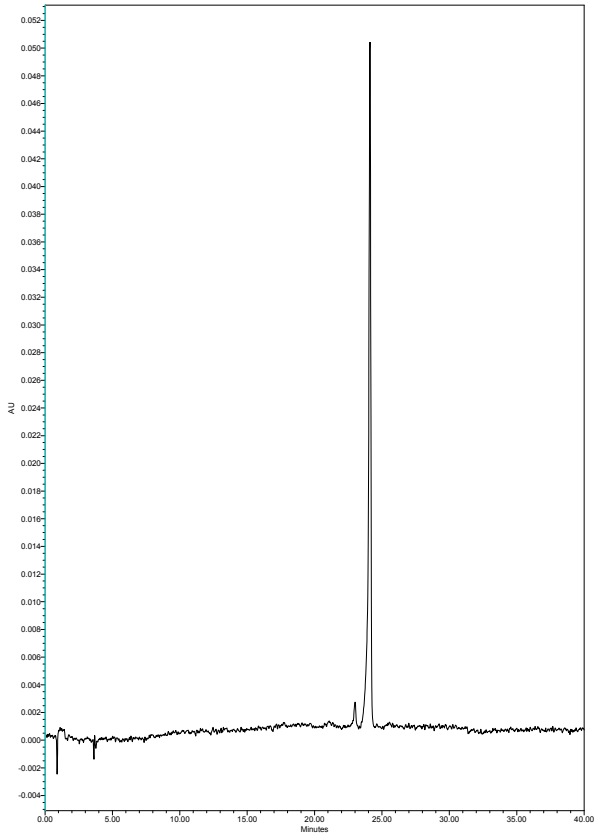

Figure S21: HPLC chromatogram profile of 1-(4'-(dimethylamino)-4-nitro-(1,1'-biphenyl)-3-yl)-2-(4'-methoxy-(1,1'-biphenyl)-4-yl) ethyl 2-(2-methoxyoctaethoxy) acetate (**11**).

UV-Visible photolysis profiles

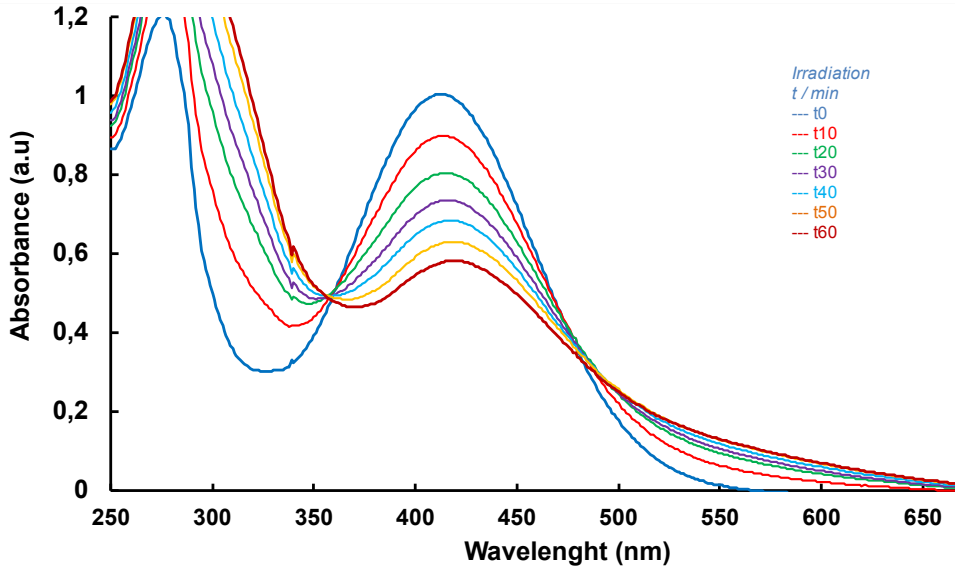

Figure S22: Variation of absorbance after irradiation: excitation at 405 nm of 135 μM solution (Acetonitrile/PBS 1:1 in vol.) of **6**.

Irradiation time (min)	% of conversion	Fluorescence integral x10^8
30	40	9.25
40	60	12.16
60	75	14.72

Table S1: Variation of fluorescence integral with irradiation time and conversion yield for **6**

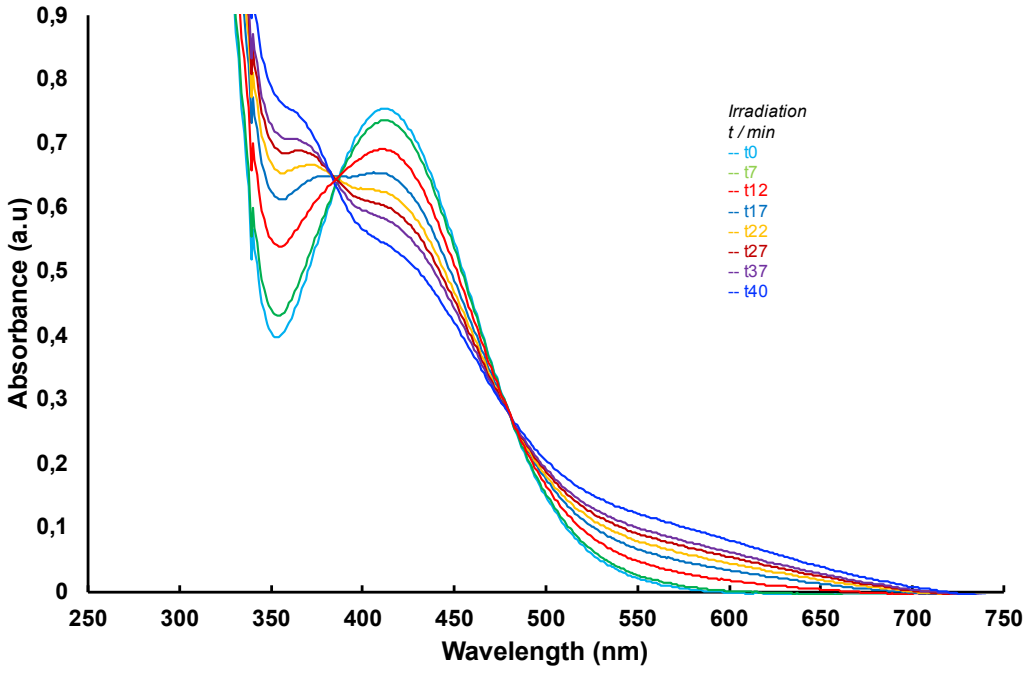

Figure S23: Variation of UV absorbance after irradiation at 405 nm of 100 μM solution (Acetonitrile/PBS 1:1 in vol.) of **7a**.

Irradiation time (min)	% of conversion	Fluorescence integral x10^8
7	30	53.46
17	40	56.14
37	55	61.08

Table S2: Variation of fluorescence integral with irradiation time and conversion yield for **7a**

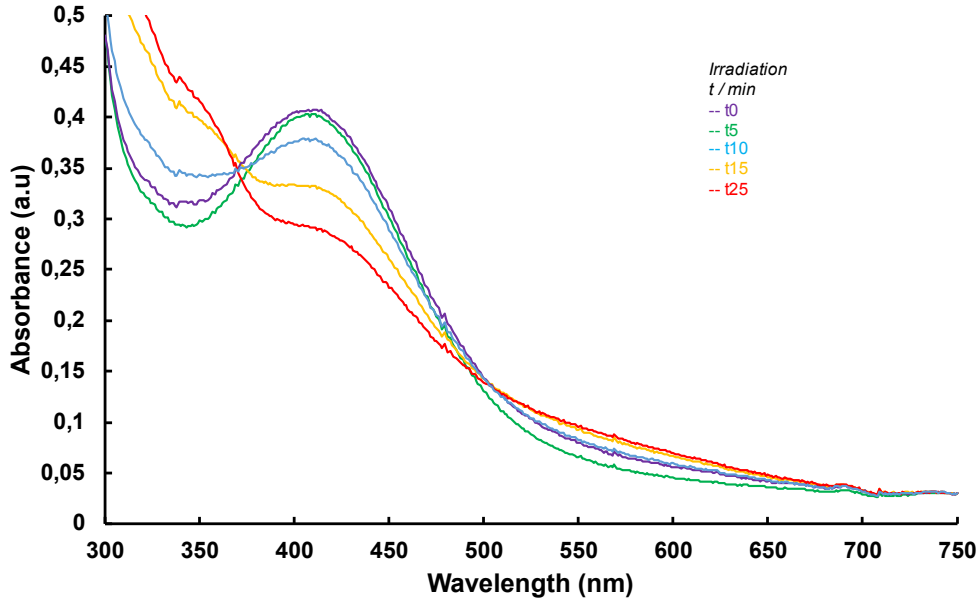

Figure S24: Variation of UV absorbance after irradiation at 405 nm of 60 μM solution (Acetonitrile/PBS 1:1 in vol.) of **7b**.

Irradiation time (min)	% of conversion	Fluorescence integral x10^8
20	20	46.84
40	35	76.53
65	55	124.36

Table S3: Variation of fluorescence integral with irradiation time and conversion yield for **7b**

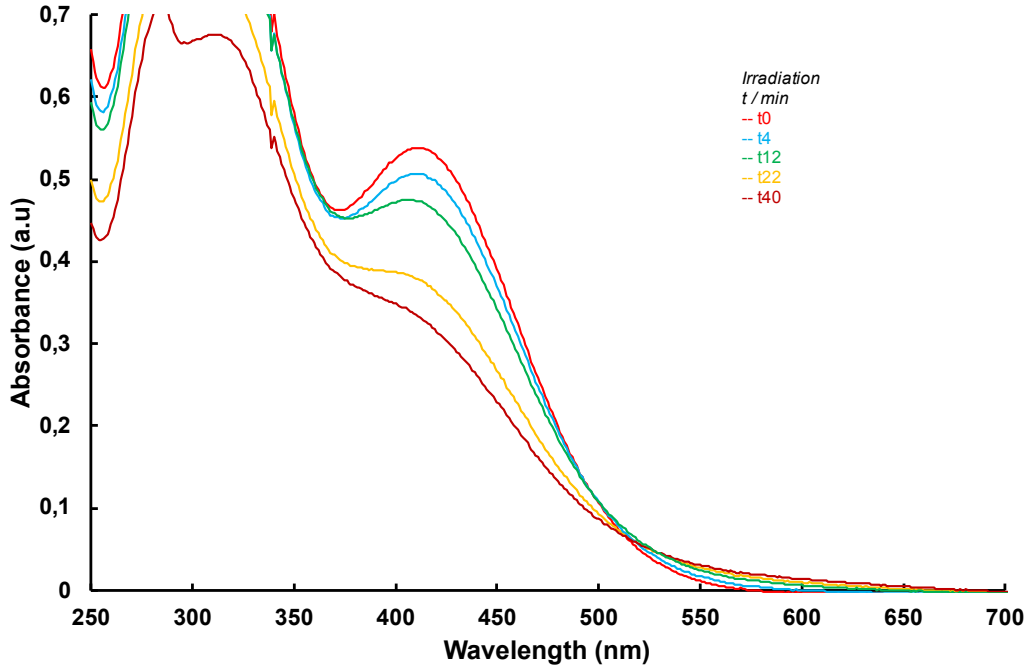

Figure S25: Variation of UV absorbance after irradiation at 405 nm of 75 μM solution (Acetonitrile/PBS 1:1) of **7c**.

Irradiation time (min)	% of conversion	Fluorescence integral x10^8
22	53	2.52
45	60	2.61
60	65	2.27

Table S4: variation of fluorescence integral with irradiation time and conversion yield for **7c**

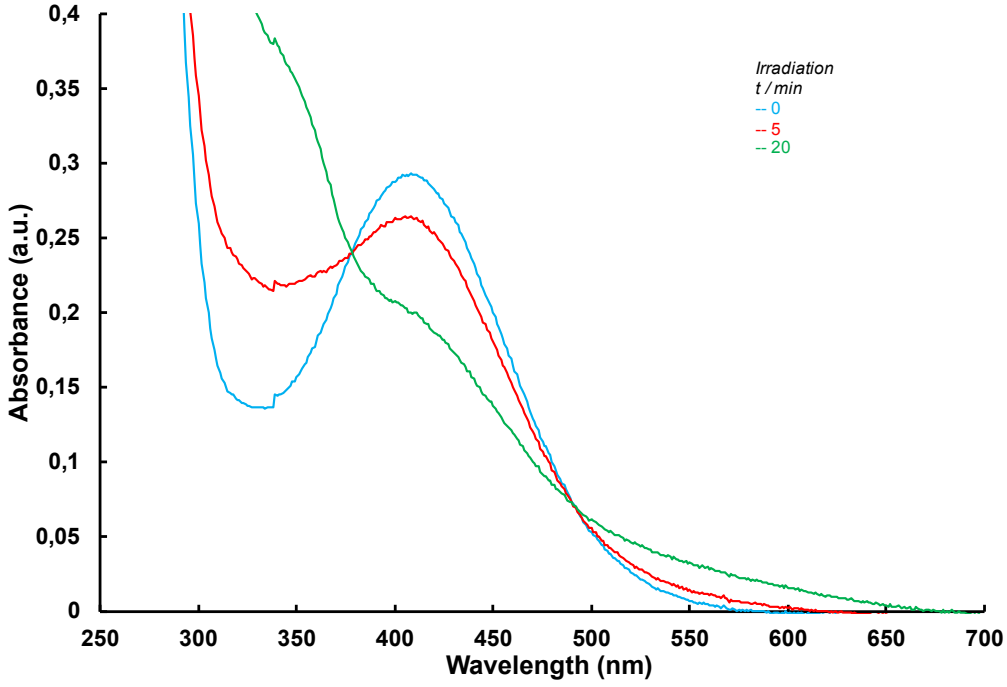

Figure S26: Variation of UV absorbance after irradiation at 405 nm of 40 μM solution (Acetonitrile/PBS 1:1 in vol.) of **11**.

HPLC calibration curve of MPAA

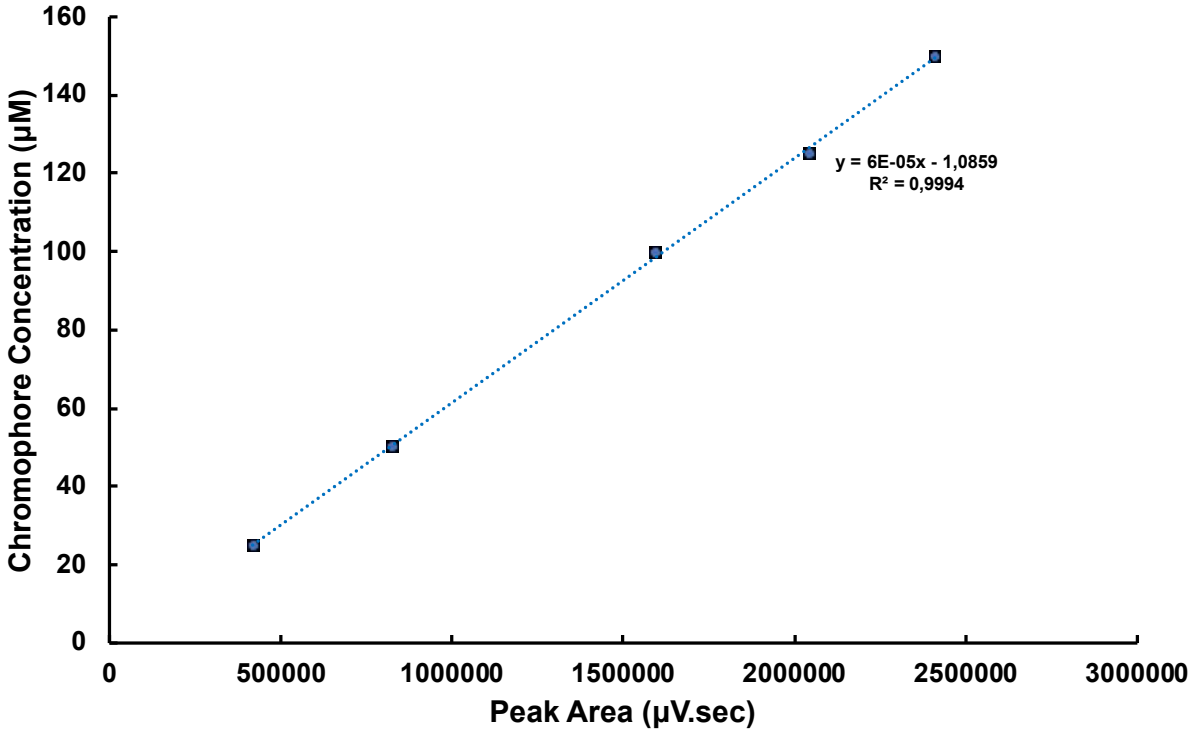

Figure S27: Calibration curve for different concentrations of the chromophore MPAA (25 μM-150 μM)

IR spectra before and after photolysis

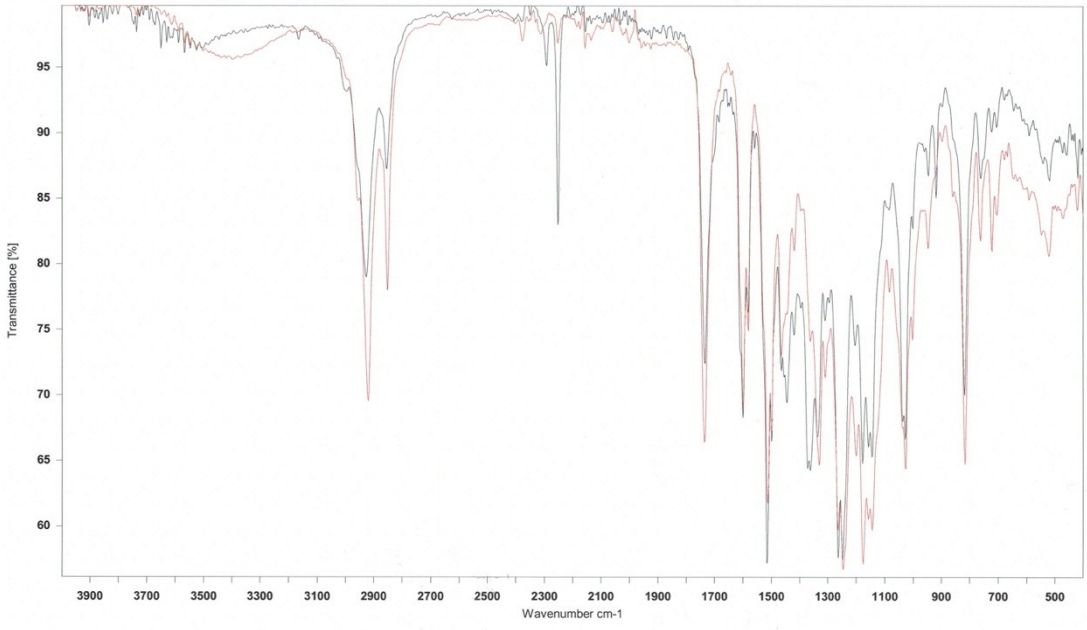

Figure S28: Infrared spectrum of the non-irradiated (red) and irradiated 40 minutes (black) samples of **7b** with concentration of 267 μM.

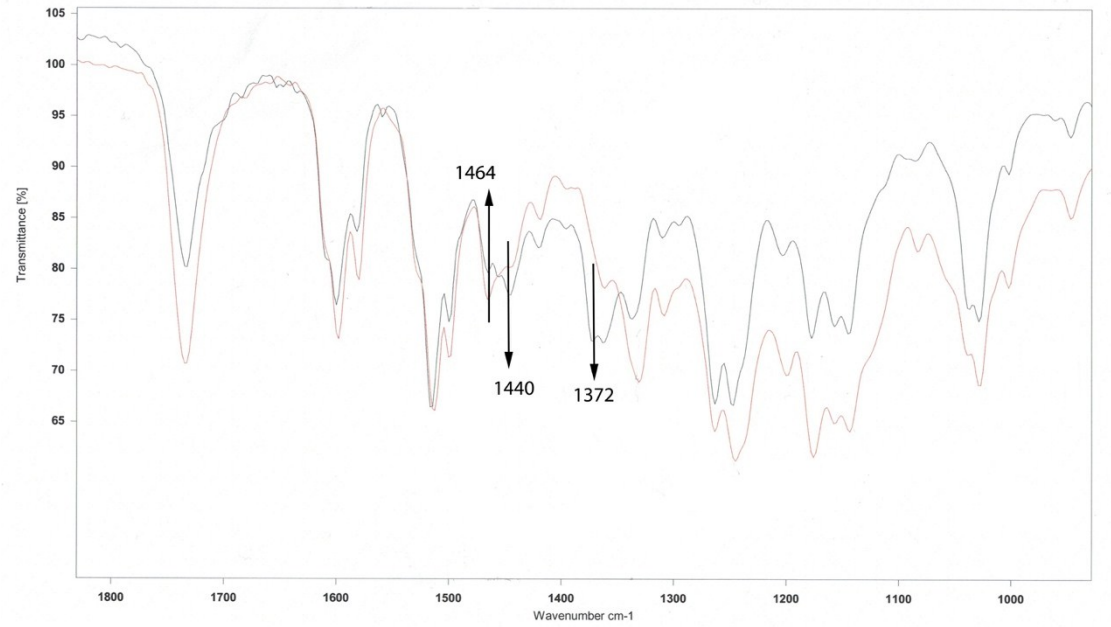

Figure S29: Infrared spectrum of the non-irradiated (red) and irradiated 40 minutes (black) samples of **7b** with concentration of 267 μM.

NMR Spectra before and after photolysis:

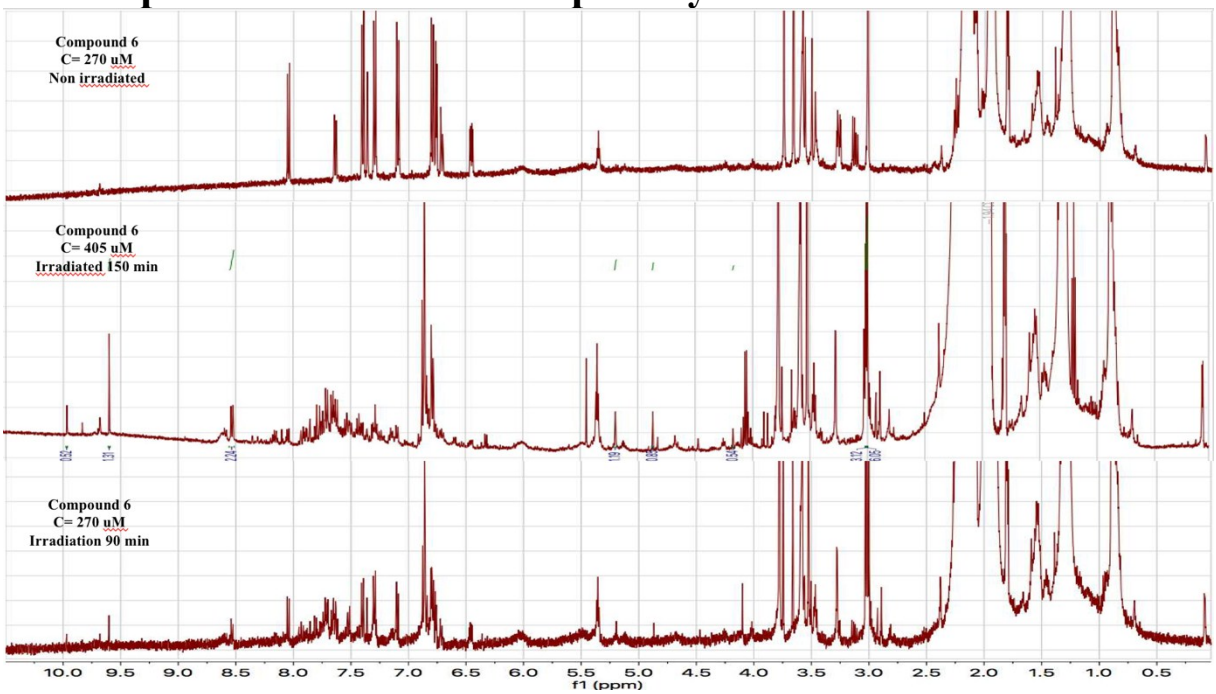

Figure S30: NMR spectra overlap of the non-irradiated (top), irradiated 405 μM solution of **6** (middle) and irradiated 267μM solution of **6** (bottom).

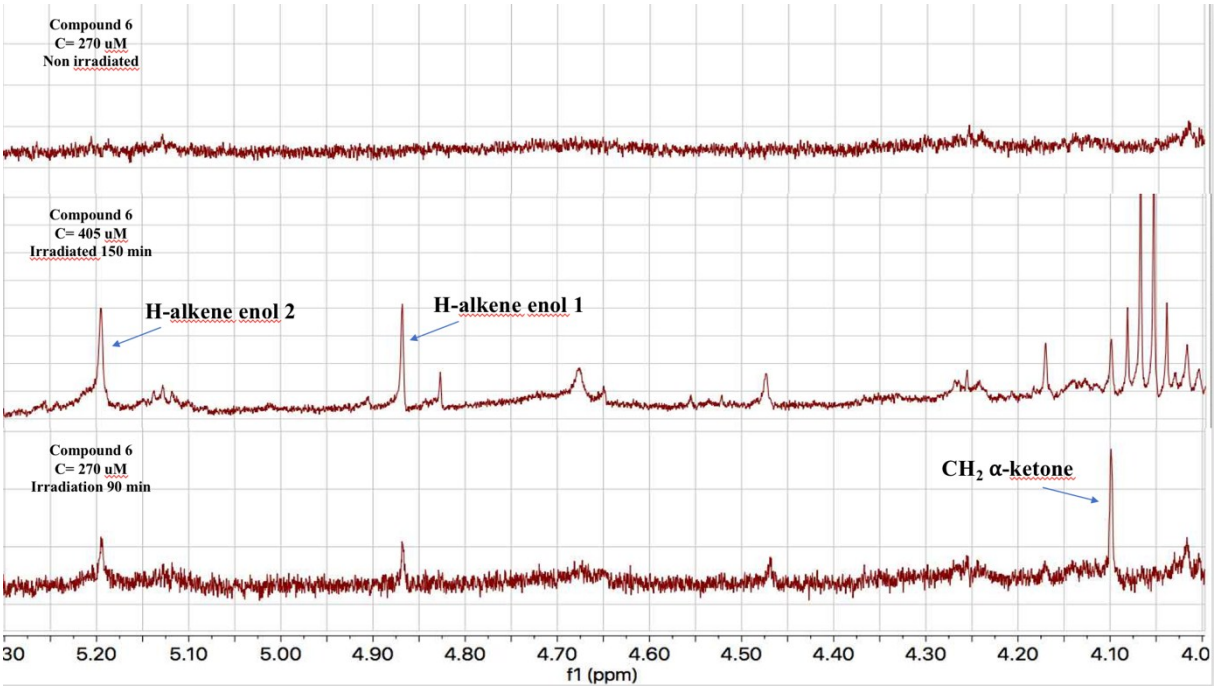

Figure S31: NMR spectra overlap of the non-irradiated (top), irradiated 405 μM solution of **6** (middle) and irradiated 267 μM solution of **6** (bottom) zone 4.0-5.3 ppm.

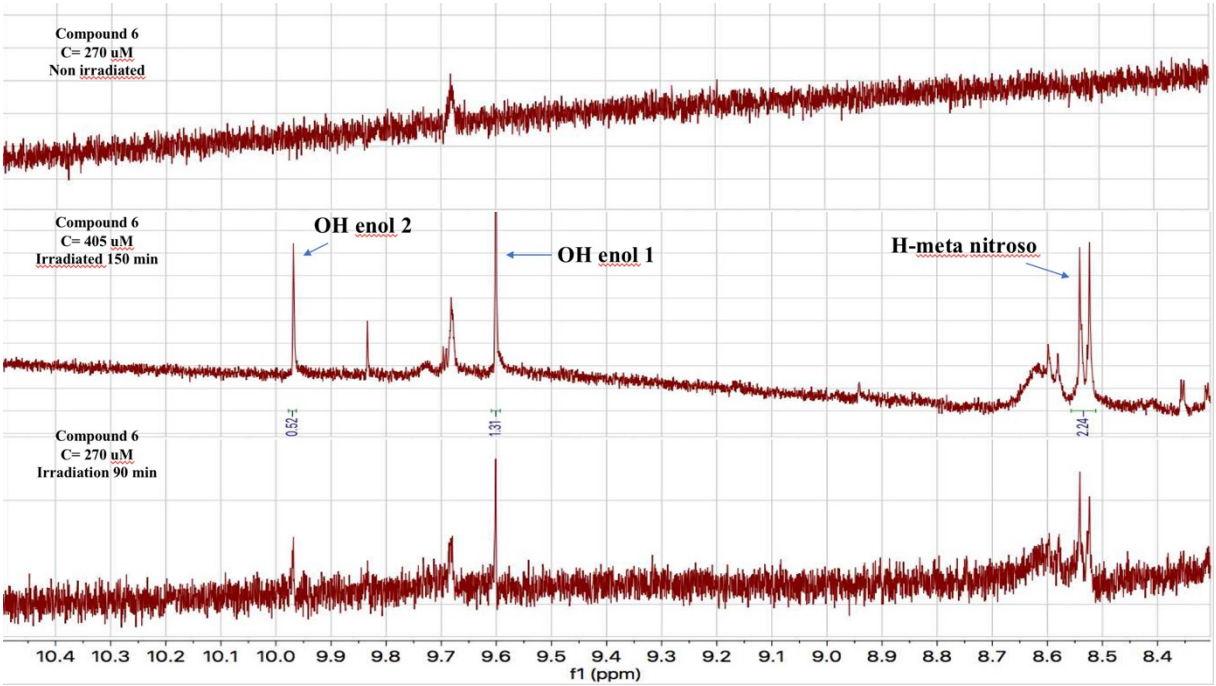

Figure S32: NMR spectra overlap of the non-irradiated (top), irradiated 405 μM solution of **6** (middle) and irradiated 267 μM solution of **6** (bottom) zone 8.5-10.5 ppm.

Photolysis on cell culture

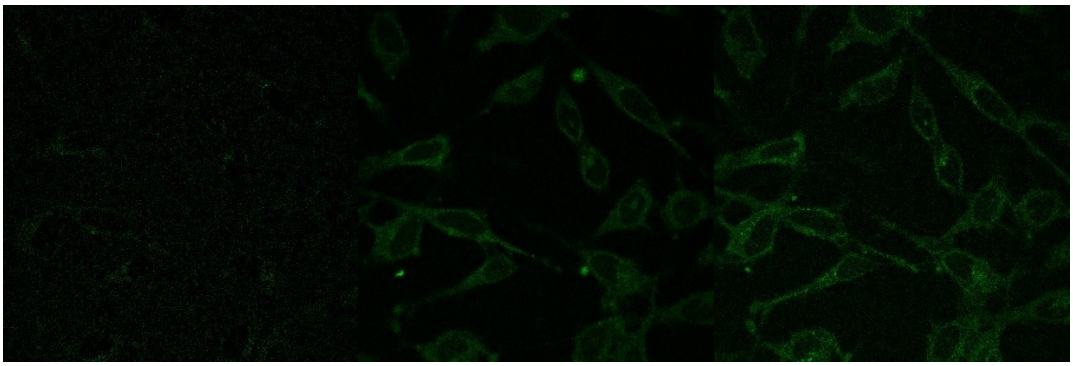

Figure S33: Fluorescence on cells without irradiation (left), 5 minutes irradiation (center) and 10 minutes irradiation (right) after incubation of **11** (1 μM)

References

1 A.M. Brouwer Pure Appl. Chem., 2011, **83 (12),** 2213–2228.
2 D. Magde, R. Wong, P.G. Seybold, Photochem. Photobiol., 2002, **75(4)**, 327-334.
3 G.A. Crosby, J.N. Demas, J. Phys. Chem., 1971, **75**, 991-1024.